NeuroImage: Clinical 16 (2017) 184–195

Contents lists available at ScienceDirect

NeuroImage: Clinical

journal homepage: www.elsevier.com/locate/ynicl

Identification of the epileptogenic zone of temporal lobe epilepsy from stereo-electroencephalography signals: A phase transfer entropy and graph theory approach

Meng-yang Wang[a], Jing Wang[a], Jian Zhou[b], Yu-guang Guan[b], Feng Zhai[b], Chang-qing Liu[b], Fei-fei Xu[a], Yi-xian Han[a], Zhao-fen Yan[a], Guo-ming Luan[b,*]

[a] Epilepsy Center and Department of Neurology, Sanbo Brain Hospital, Capital Medical University, Beijing Key Laboratory of Epilepsy, Beijing Institute for Brain Disorders, 50, Xiang-shan-yi-ke-song, Haidian District, Beijing 100093, China

[b] Epilepsy Center and Department of Functional Neurosurgery, Sanbo Brain Hospital, Capital Medical University, Beijing Key Laboratory of Epilepsy, Beijing Institute for Brain Disorders, 50, Xiang-shan-yi-ke-song, Haidian District, Beijing 100093, China

ARTICLE INFO

Keywords:
Temporal lobe epilepsy
Stereo-electroencephalography
Phase transfer entropy
Graph theory
Epileptogenic zone
Surgical outcome

ABSTRACT

The aim of this research is to apply an approach based on phase transfer entropy (PTE) and graph theory to study the interactions between the stereo-electroencephalography (SEEG) activities recorded in multilobar origin, in order to evaluate their ability to detect the epileptogenic zone (EZ) of temporal lobe epilepsies (TLE). Forty-three patients were included in this retrospective study. Five to sixteen (median = 12) multilead electrodes were implanted per patient, and, for each patient, a sub-set of between 10 and 32 (median = 22) bipolar derivations was selected for analysis. The leads were classified into the onset leads (OLs), the early propagation leads (EPLs), and the rest of the leads (RLs). The results showed that a significantly different dynamic trend of the out/in ratio (more obvious in the gamma band) distinguishes the OLs from RLs in the 23 patients who were seizure-free not only during the ictal event (significant elevation), but also during the inter-,pre-, late-ictal periods, and especially in the post-ictal (sharp decline) state. However, in the 20 patients who were not-seizure-free, the differences between the OLs and RLs during the post-ictal period were not found in any frequency band. The dynamic trend was used to predict surgical outcome, and the results showed that the sensitivity was 91% and the specificity was 70%. In brief, this study indicates that our approach may add new and valuable information, providing efficient quantitative measures useful for localizing the EZ.

1. Introduction

Temporal lobe epilepsy (TLE) is the most common type of pharmacoresistant epilepsy in adults, and it is frequently successfully treated by surgery, although long-term relapses in up to 58% of cases suggest insufficient network disruption (Coito et al., 2015). Although it primarily affects the temporal lobes, TLE is thought to be a network disease with widespread extratemporal effects. One or both hippocampi are commonly involved in TLE, and this is often visible as hippocampal sclerosis on structural MRI. Hippocampal involvement can also occur in TLE without hippocampal sclerosis in neocortical TLE, in temporal 'plus' epilepsies, and even in extra-temporal epilepsies (Barba et al., 2007; Haneef et al., 2014).

In most TLE with hippocampal sclerosis, the extent of the surgical resection can be defined by noninvasive presurgical investigation (Gnatkovsky et al., 2014). Nonetheless, the identification of epileptogenic zone (EZ) boundaries in patients with equivocal TLE and in imaging negative cases requires invasive recordings. However, stereo-electroencephalography (SEEG) registers electrical activity from a very confined region, and this may lead to false localization of the ictal onset zone. This is likely if there is no clear distinction among ictal onset patterns corresponding either to the ictal onset zone proper or to areas of ictal spread (Singh et al., 2015).

The EZ represents the minimum amount of cortex that must be resected (inactivated or completely disconnected) to achieve seizure freedom (Panzica et al., 2013). The non-negligible rate of failure in epilepsy surgery brings evidence that the question of the definition of the EZ is still unsolved and that progress must still be made to determine the epileptogenicity of the brain regions in a patient-specific context (Bartolomei et al., 2008).

* Corresponding author at: Guo-ming Luan, MD, PhD, Epilepsy Center and Department of Functional Neurosurgery, Sanbo Brain Hospital, Capital Medical University, Beijing Key Laboratory of Epilepsy, Beijing Institute for Brain Disorders, 50, Xiang-shan-yi-ke-song, Haidian District, Beijing 100093, China.
E-mail address: luanguoming2016@sina.com (G.-m. Luan).

http://dx.doi.org/10.1016/j.nicl.2017.07.022
Received 3 February 2017; Received in revised form 15 June 2017; Accepted 22 July 2017
Available online 24 July 2017

The visual inspection of SEEG signals does not allow full advantage to be taken of the intrinsic properties of the epileptogenic network, so more sophisticated diagnostic methods are required (Varotto et al., 2012). Phase transfer entropy (PTE) is a novel, information theory–-based measure of directed connectivity. It exhibits many characteristics that make it especially suitable for connectomics analysis of electroencephalography (EEG) data (Lobier et al., 2014; Dauwan et al., 2016).

However, regardless of the method used to evaluate connectivity, such an approach may not be sufficient to grasp the full complexity of the brain as a network (Varotto et al., 2012). Graph theory (Boccaletti et al., 2006) is currently widely used to analyze the structure and evolution of complex networks in a quantitative manner (Varotto et al., 2012; Stam, 2014). In recent years, some efforts have been made to develop the approach based on graph theory for improving the identification of the EZ, since the study of the topological properties of the networks has strongly improved the study of brain connectivity mechanisms (Panzica et al., 2013). However, these are still qualitative studies (Varotto et al., 2012; Wilke et al., 2010; Van Mierlo et al., 2013; Antony et al., 2013).

In this study, we apply a quantitative approach based on PTE and graph theory to study the dynamics of the interactions between the SEEG activities recorded in the multilobar origins, which are characterized by the involvement of a complex epileptogenic network of a group of patients with TLEs, to evaluate their ability to detect the EZ. Our primary hypothesis is that the electrical net outflow of epileptogenic zone in gamma band changes dynamically from the inter-, pre-, early- and late-ictal periods to the post-ictal period, especially rise in the early-ictal section and decline in the post-ictal section. Our minor hypothesis is that the above-mentioned regularity should be tenable regardless the types of TLEs and the types of SEEG onset patterns, but the details may be different.

2. Material and methods

The study was approved by the ethics committee of Sanbo Brain Hospital, Capital Medical University, where it was carried out from May 2015 to December 2016. Informed consent was obtained from the patients or legal guardians.

2.1. Patients

Subjects for this retrospective study included patients with drug-resistant focal seizures of suspected temporal lobe origin at the Sanbo Brain Hospital in Beijing between January 2012 and January 2016, and who were candidates for epilepsy surgery but required diagnostic depth electrode studies because results from non-invasive tests were inconclusive.

All patients had a comprehensive evaluation, including detailed history and neurological examination, neuropsychological testing, routine magnetic resonance imaging (MRI), surface EEG, seizure semiolgoy and SEEG. Patients were selected for the present study if they satisfied the following criteria: (i) absence of any detectable lesion at mesial temporal lobe on MRI, with the exception of hippocampal sclerosis; (ii) no history of epilepsy surgery; (iii) SEEG recordings showing that seizures involved at least mesial and/or neocortical temporal lobe structures; (iv) surgery performed according to SEEG results, taking into account anatomical constraints; and (v) at least 1 year of postoperative follow-up. According to the criteria, 43 patients with drug-resistant TLE were selected from a series of 180 cases. Five to sixteen (median = 12) multilead electrodes were implanted per patient in temporal and extratemporal areas, depending on the suspected origin and region of early spreading of seizures.

The population consisted of 24 males and 19 females, aged 12.2–39.4 years (see the clinical findings in Table 1). Epilepsy-onset age ranged from 1 to 31 years. Eight patients (29%, 8/28) with mesial TLE and one patient (7%, 1/15) with neocortical TLE had experienced febrile convulsions in childhood. Four patients (14%, 4/28) with mesial TLE and eight patients (53%, 8/15) with neocortical TLE had normal MRI scans.

Hippocampal sclerosis was identified radio-graphically and later confirmed pathologically in 17 cases with mesial TLE without early extratemporal propagation (74%, 17/23), 0 case in the patients with the other types of TLEs. One case with mesial TLE and one case with neocortical TLE showed hippocampal sclerosis on MRI, but this could not be confirmed pathologically. One case showed pathological hippocampal sclerosis, which was not identified radio-graphically. Different types of anatomical lesions were found in 24 cases, including 1 ganglioglioma, 2 type IIb focal cortical dysplasias (FCD), 3 type IIa FCDs, 10 type Ib FCDs, 2 type Ia FCDs, and 6 other lesions.

The seizure-onset zone (SOZ) was defined as the depth electrode contacts showing the first unequivocal ictal intracranial EEG change. Seizure early propagation was defined as a clear seizure discharge, starting 0.5–5 s after seizure onset and recorded outside the SOZ (Perucca et al., 2014). There were 20 patients who had early propagation on SEEG after seizure onset. Four ictal onset patterns were identified across the 43 seizures: low-voltage fast activities (12 cases, 28%); low-frequency high-amplitude periodic spikes (11 cases, 26%); spike or polyspike fast discharges (15 cases, 33%); and spike- or sharp-and-wave rhythmic activities (5 cases, 12%).

In the 25 patients with mesial TLE, surgery consisted of a tailored resection, including at least the temporal pole and mesio-temporal lobe structures (amygdala, hippocampus, and para-hippocampal gyrus). The posterior limits of the temporal neocortical resection varied according to SEEG results. A selective amygdalo-hippocampectomy was performed in the other three patients (No. 1, 21 and 24) with mesial TLE, and two (No. 21 and 24) patients with mesial TLE with early extratemporal propagation were operated on twice, since seizures recurred rapidly. In the 15 patients with neocortical TLE, individualized surgical planning was performed according to SEEG and imaging results, and one (No. 37) of the patients with neocortical TLE with early extratemporal propagation underwent two episodes of electrode implantation and two operations.

Postoperative seizure status, according to Engel's classification (Engel, 1993), showed that 20 mesial TLE patients without early extratemporal propagation were in class I (87%, 20/23), whereas only 1 mesial TLE patient with early extratemporal propagation was in class I (20%, 1/5); 5 neocortical TLE patients without early extratemporal propagation were in class I (63%, 5/8), whereas 3 neocortical patient with early extratemporal propagation was in class I (43%, 3/7); and 10 patients with low-frequency high-amplitude periodic spikes (91%) and 13 (80%) with spike or polyspike fast discharges were in class I, whereas only 5 with low-voltage fast activities (50%) and 1 with spike- or sharp-and-wave rhythmic activities (20%) were in class I.

2.2. SEEG recordings

The SEEG exploration was performed using intracerebral multiple-contact electrodes (Huake-Hengsheng Medical Technology, China; 8–16 contacts, length: 2 mm, diameter: 0.8 mm, 1.5 mm apart) placed intracranially with the aid of a stereotactic ROSA robotic device (Medtech). The SEEGs were recorded using a common reference electrode (Nicolet™ system; 128-channels; sampling rate: 512 Hz). The SEEG recording was carried out during long-term video-EEG monitoring to record several of the patient's habitual seizures, following complete or partial withdrawal of antiepileptic drugs. We used bipolar derivation to avoid possible contamination deriving either from a not completely inactive common reference or from interference due to a volume conduction effect.

A patient management conference was then held for each individual, after enough seizures were recorded (at least three to five seizures), to discuss the results and implications of the SEEG study and to decide collectively on a plan for resection. Subsequent to this

Table 1
Clinical patient characteristics, presurgical evaluations, and surgical outcome.

No.	Sex	Age (yr)	Feb szr	Epi on (yr)	Aura	Epi side	MRI data		Epileptogenic zone		Ictal pattern	Early propagation & complete resection	Reg	Postop class
							HS	NAL	MTL	NTL				
1	F	26.8	−	4	Vis + Aud	R	RD	−	+	−	LFPS	–	OR	IB
2	M	13.7	−	4	Aud + Fear + Drm	L	–	−	−	+	LVFA	–	NOR	IVA
3	M	24.9	−	12	Vis + Headache	L	LD	+	+	−	LFPS	–	OR	IA
4	F	36.2	−	26	–	L	–	−	+	−	LVFA	LTL + BTL(3–4 s), Res	NOR	IIA
5	F	23.5	−	1	Fear	L	L	−	+	−	LFPS	PHc (< 1 s), Res	OR	IA
6	M	18.2	−	12	Diz + Aud	R	–	−	−	+	LVFA	TPO (1–4 s), NRes	OR	IA
7	M	19.6	−	11	Diz	R	–	−	−	+	SpRA	MTL + PCu(2 s), NRes	OR + RR	IIB
8	M	21.5	+	6	Djv	R	RD	+	+	−	SpFD	Tp (2 s), Res	OR	IA
9	M	25.8	−	21	–	R	–	−	+	−	LVFA	Ins (0.5–1 s) + CMTL (3 s), NRes	NOR	IIA
10	M	25.5	−	12	–	R	R	−	+	−	SpRA	–	OR	IA
11	M	26.9	+	8	–	L	L	+	+	−	SpFD	LTL + BTL (2–4 s), Res	OR	IA
12	M	16.4	−	7	Abdominal	R	–	+	−	+	LVFA	MFG (< 1 s), NRes	NOR	IVB
13	M	39.5	−	7	Fear	L	L	+	+	−	LFPS	–	OR	IB
14	M	12.3	−	7	Fear	R	–	+	−	+	SpFD	–	OR	IA
15	F	25.4	−	21	–	L	–	−	+	−	SpRA	Ins (< 1 s), NRes	OR + RR	IIIA
16	M	37.4	+	15	Aud	R	–	−	−	+	SpFD	–	OR	IA
17	M	29.5	−	6	Som	R	–	+	−	+	SpFD	Ins + LTL(< 1 s), Res	OR	IIA
18	F	21.8	+	14	–	R	R	+	+	−	LFPS	–	NOR	IB
19	F	29.2	−	4	Abdominal + Vis	R	R	−	+	−	SpFD	–	OR + RR	IA
20	F	26.0	−	11	–	R	L	−	−	−	LVFA	AnG + MTL (4–5 s), NRes	NOR	IA
21[a]	F	28.2	−	26	Cephalic	L	–	+	+	−	SpRA	Ins (< 1 s), NRes	OR + PR	IVA
22	F	21.7	−	16	Pal	L	–	−	+	−	SpFD	BTL + LTL (0.5–4 s), Nres	OR + PR	IA
23	M	22.6	+	12	Som	R	R	−	+	−	LFPS	–	OR	IA
24[b]	M	14.6	−	9	Vis	L	–	−	+	−	SpFD	PCG + LG (1 s), NRes	OR	IIA
25	M	27.7	+	3	Vis	L	L	+	+	−	LVFA	–	NOR + RR	IC
26	M	30.9	−	19	–	L	–	+	−	+	LVFA	BTL + MTL (< 1 s), Res	OR	IA
27	F	21.6	−	14	Diz	R	R	−	+	−	LVFA	MTL (< 1 s), Res	OR	IA
28	M	18.8	−	3	Headache + Vis	R	–	+	−	+	SpFD	–	OR	IA
29	F	15.0	−	12	Aud + Som	L	–	−	−	+	SpRA	–	OR + RR	IVA
30	F	29.0	+	17	Fear	R	R	−	+	−	LFPS	–	OR	IA
31	F	32.6	−	16	Djv	R	R	−	+	−	LFPS	MTL (1–2 s), Res	NOR	IB
32	F	26.7	−	4	Pal	L	L	+	+	−	SpFD	–	NOR + RR	IB
33	M	37.1	−	18	–	L	–	+	−	+	SpFD	Fop (3 s), NRes	OR	IA
34	M	16.7	−	4	–	L	–	+	+	−	SpFD	MTL + Ins + LTL (< 1 s), NRes	OR	IA
35	F	22.9	−	15	–	L	LD	+	+	−	LFPS	–	OR	IA
36	M	26.6	−	14	–	L	–	−	−	+	LVFA	–	OR	IA
37[c]	F	25.0	−	10	Aud	R	–	−	−	+	LVFA	SmG (< 1 s) + MTL (4 s), NRes	NOR	IVB
38	F	24.8	−	12	Fear	R	–	−	+	−	LFPS	–	OR	IA
39	F	21.0	−	5	Abdominal	R	R	−	+	−	LFPS	–	NOR	IVB
40	M	31.7	−	29	–	L	–	+	+	−	SpFD	–	OR	IA
41	M	27.9	+	11	Pal	L	L	−	+	−	SpFD	–	OR	IA
42	F	37.8	+	31	Fear + Pal + Djv + Diz	R	R	−	+	−	SpFD	–	OR + RR	IVB
43	M	12.6	−	9	Aud + Som	L	–	−	−	+	LVFA	–	OR	IVB

[a, b, c] seizure free after the second epilepsy surgery; Feb szr = febrile seizure; Epi on = age at epilepsy onset; HS = Hippocampal sclerosis; NAL = neocortical anatomical lesion; MTL = mesial temporal lobe; NTL = neocortical temporal lobe; Postop class = seizure outcome according to Engel's classification; Vis = visual; Aud = auditory; Drm = dreaming state; Som = somatosensory; Pal = palpitation; Djv = Déjà vu; Diz = dizziness; R = right; L = left; RD = right dominant (bilateral); LD = left dominant (bilateral); LFPS = low-frequency high-amplitude periodic spikes; LVFA = low-voltage fast activity; SpFD = spike or polyspike fast discharges; SpRA = spike- or sharp-and-wave rhythmic activity; LTL = lateral temporal lobe; BTL = basal temporal lobe; PHc = parahippocampus; TPO = temporo-parieto-occipital junction; PCu = precuneus; TP = temporal pole; Ins = insula; AnG = angular gyrus; CMTL = contralateral mesial temporal lobe; MFG = middle frontal gyrus; PCG = posterior cingulate gyrus; LG = lingual gyrus; Fop = frontal operculum; SmG = Supramarginal gyrus; Res = complete resection; NRes = not complete resection; Reg = regularity; OR = the onset leads meet the regularity that the out/in ratio in the 30–80-Hz band during the early-ictal period is more than that during the post-ictal and pre-ictal periods, and this ratio is no < 1.10; NOR = the onset leads do not meet the above mentioned regularity; PR or RR = the early propagation leads or the rest of the leads meet the above mentioned condition and the correlation coefficient of the out/in ratio between these leads and the most marked onset lead is no < 0.5.

meeting and approximately 8–12 weeks after removal of the SEEG electrodes, patients underwent a standard craniotomy for tailored resection of the hypothetical EZ.

2.3. Data selection and signal analysis

From seizure recordings, an expert electroencephalographist selected the most significant seizure for the identification of the EZ. Although more than one seizure was available in some patients, only

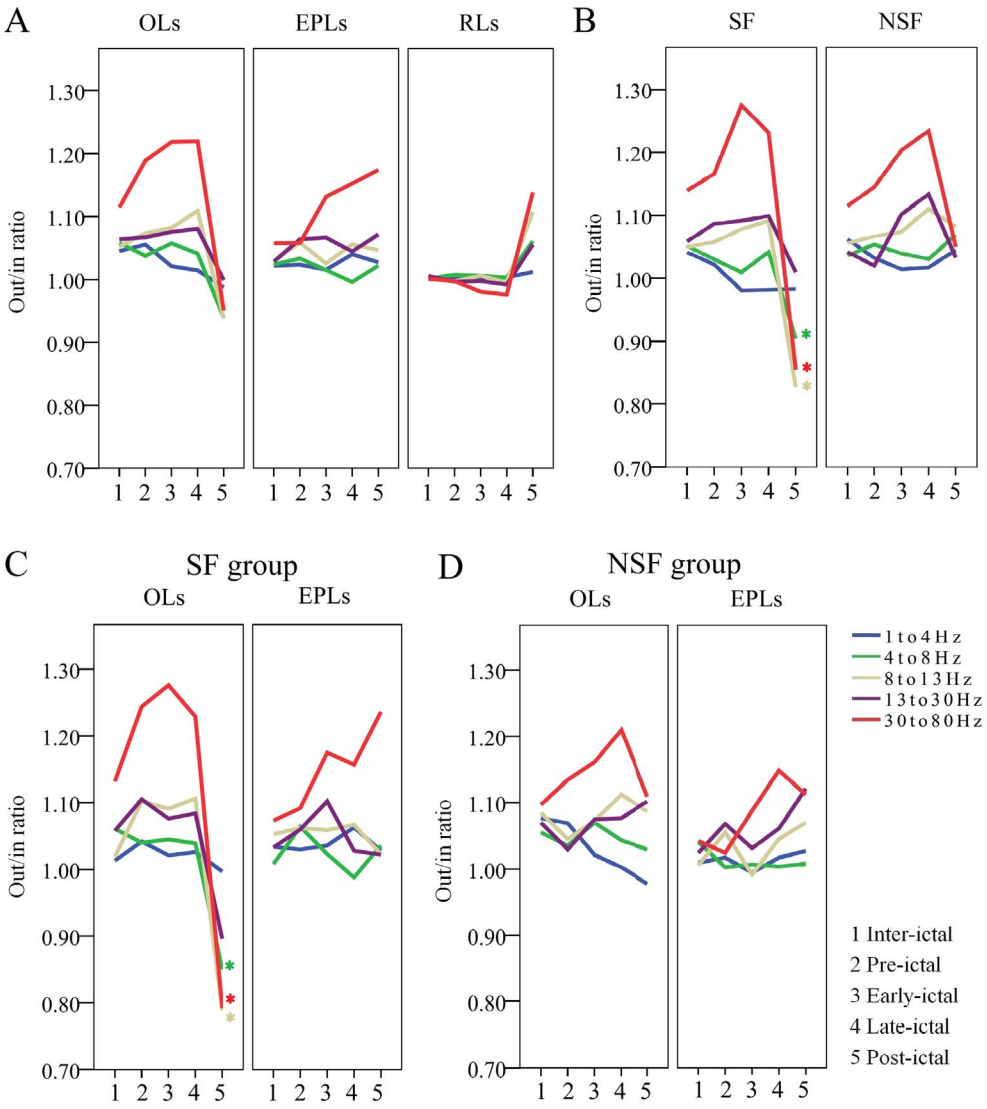

Fig. 1. Dynamic changes of the out/in ratio.
A. Out/in ratio analysis according to the site of the leads. OLs = the onset leads; EPLs = the early propagation leads; RLs = the rest of the leads.
B. Out/in ratio differences between the seizure-free (SF) and not-seizure-free (NSF) groups. Green *: 4–8 Hz, p = 0.015; gray *: 8–13 Hz, p = 0.015; red *: 30–80 Hz, p = 0.044.
C. Out/in ratio differences between the OLs and EPLs in the SF group. Green *: 4–8 Hz, p = 0.023; gray *: 8–13 Hz, p = 0.043; red *: 30–80 Hz, p = 0.029.
D. Out/in ratio differences between the OLs and EPLs in the NSF group.

one seizure (sufficiently long and stationary enough for the analysis) was selected, to avoid statistical bias. The secondary generalized tonic and clonic seizures were excluded because diffused postictal electrical silence would last a longer time. In addition, recordings were chosen at least 2 days after the electrode implantation surgical procedure to limit the possible effect of the general anesthesia.

For each patient, a subset of between 10 and 32(median = 22)bipolar derivations was selected for analysis: (i) The leads inside the seizure onset and early propagation regions must be selected first, followed by (ii) the leads inside the mesial TL and neocortical TL, and (iii) the leads inside the orbito-frontal cortex, insula, operculum, temporo–parieto–occipital junction, etc.

The SEEG recordings were divided into five temporal sections: inter-ictal, pre-ictal (before seizure onset), early-ictal (initial seizure onset), late-ictal (subsequent to appearance of the rapid discharges after early-ictal), and post-ictal (just after seizure termination). Four periods of 8 s (one epoch) were analyzed during pre-ictal, early-ictal, late-ictal, and post-ictal sections in each patient. For the inter-ictal state, 10 consecutive epochs of 80 s in an awake state were analyzed. Artifact-free epochs were visually selected for each subject.

2.4. Phase transfer entropy and graph theory-based measures

Before estimating PTE, the SEEG data were pre-processed by a 50-Hz notch filter, used to suppress the noise of the electrical power line. Selected epochs were converted to ASCII files for further analysis with the BrainWave software (Version: 0.9.152.4.1). The signal was digitally filtered in different frequency bands: delta (1–4 Hz), theta (4–8 Hz), alpha (8–13 Hz), beta (13–30 Hz), and gamma (30–80 Hz). PTE for a given analysis lag δ is defined as (Lobier et al., 2014):

$$\text{Phase TE}_{x-y} = H(\theta_y(t), \theta_y(t')) + H(\theta_y(t'), \theta_x(t')) - H(\theta_y(t), \theta_y(t'), \theta_x(t'))$$

$\theta_x(t')$ and $\theta_y(t')$ are the past states at time point $t' = t - \delta$: $\theta_x(t') = \theta x(t - \delta)$ and $\theta y(t') = \theta y(t - \delta)$).

For the inter-ictal section, PTE and the related directed and weighted matrix were estimated for each epoch of 8 s in each frequency band, and then averaged over the section. Graph theoretical measures were applied to the PTE matrices to examine the network topology of the directed connections of each band in all five temporal sections between the contacts. The simplest quantitative index of a node is the degree, which indicates the total number of connections either from (in-degree) or toward (out-degree) all the other vertices and represents the most common measures of centrality. As the number of network nodes of each patient varied, the ratio between the out-degree and in-degree (out/in ratio) was used to ensure a correct group analysis. There was no obvious correlation ($|r| < 0.4$, $p > 0.05$) between the quantity of the electrodes and the values of the out/in ratio in this study. In-degree and

out-degree are defined as:

$$k_{in}(i) = \frac{\sum_{j \in V} a_{ij}}{n}$$

$$k_{out}(i) = \frac{\sum_{j \in V} a_{ji}}{n}$$

The PTE related matrix was converted to .net file format (Pajek readable) using a custom written toolbox in MATLAB R2014a, and then the .net file was opened by Gephi0.8.2, a network visualization software used in various disciplines, with which out-degree and in-degree were calculated and a circle graph was drawn.

2.5. Statistical analysis

A non-parametric Mann–Whitney test was performed to compare values of the out/in ratio between the two groups of patients, and a Kruskal–Wallis *t*-test was performed to compare three or more groups of sample data (multiple comparisons were performed, and all the significant p values were adjusted). Correlation between out/in ratio values was made using a non-parametric measure of correlation (Spearman's rank correlation coefficient). Statistical comparisons were made using either Fisher's exact test or χ^2 tests for categorical variables. A p value < 0.05 was considered as significant.

3. Results

3.1. Out/in ratio analysis according to the site of the leads

The out/in ratio was evaluated first in the 20 patients in whom one to several electrodes demonstrated early propagation EEG patterns. The results showed that the onset leads (OLs), the early propagation leads (EPLs), and the rest of the leads (RLs) were characterized by different dynamic trends. A Mann–Whitney test showed significant differences both between the OLs and RLs and between the EPLs and RLs in the three frequency bands (8–13 Hz, 13–30 Hz, and 30–80 Hz) in most of the temporal sections. A significant difference between the OLs and EPLs was only found in the gamma band in the pre-ictal section (Fig. 1A and Table 2).

In the 23 patients with seizure-free, most of the differences between the OLs and RLs were similar to the above-mentioned results. However, a significant decline of the out/in ratio observed in the OLs during the post-ictal period was not found in the not-seizure-free group (Table 2).

A further comparison of the OLs between the seizure-free and not seizure free groups showed that the differences were only in the 4–8-Hz ($p = 0.015$), 8–13-Hz ($p = 0.015$), and 30–80-Hz ($p = 0.044$) frequency bands during the post-ictal state (Fig. 1B).

A further comparison of the out/in ratio between the OLs and EPLs was made in the seizure-free and not-seizure-free patients, respectively, to clarify the epileptogenicity of early propagation. The results showed that the EPLs of the seizure-free group (10 cases) had a significantly higher out/in ratio than the OLs in the 4–8-Hz ($p = 0.023$), 8–13-Hz ($p = 0.043$), and 30–80-Hz ($p = 0.029$) frequency bands under the postictal condition. These differences were not found in the not-seizure-free group (10 cases) (Fig. 1C and D). Appearance of the early propagation or complete resection of the regions showing this EEG pattern did not relate to the surgical outcome ($p = 0.669$ and 0.370 respectively), despite excluding the cases ($p = 0.266$) with an atypical dynamic trend of the out/in ratio in the OLs. However, the much earlier extratemporal propagation (within 3 s) suggested a significantly bad outcome (Fig. 2 A, B, C, D, and E). A further analysis of the surgical outcome according to the out/in ratio of the early propagation was not made, because of a small sample size.

There were 6 patients aged between 12.3 and 16.7 years old in our study. We made additional statistics, and found that it did not strongly influence the results after outlier removal of these adolescent patients.

3.2. Out/in ratio differences among the frequency bands

The Kruskal–Wallist multiple comparison test showed that, in the 23 seizure-free cases, the out/in ratio of the OLs in the gamma band was significantly higher than those in the delta and theta band during pre-ictal period ($p = 0.000$ and 0.008), higher than those in all the other bands during early-ictal period ($p = 0.000$, 0.000, 0.004 and 0.028), and higher than those in all the other bands during late-ictal period ($p = 0.000$, 0.000, 0.002 and 0.005). In the 20 not-seizure-free cases, the superiority ($p < 0.05$) of the gamma band was only observed in the comparisons with the delta and theta bands in the pre-ictal, early-ictal and late-ictal periods. The EPLs (20 cases) only showed the superiority in the gamma band in the comparisons with the delta ($p = 0.000$), theta ($p = 0.001$) and beta bands ($p = 0.041$) in the late-ictal section.

3.3. Dynamic changes of out/in ratio in chronological order

The Kruskal–Wallist multiple comparison test showed that, in the 23 seizure-free cases, the significant fluctuations in the out/in ratio of the OLs mainly in the theta (inter-ictal vs. post-ictal: $p = 0.016$), alpha (early-ictal vs. post-ictal: $p = 0.039$; late-ictal vs. post-ictal: $p = 0.006$), and gamma (inter-ictal vs. post-ictal: $p = 0.030$; pre-ictal vs. post-ictal: $p = 0.011$; early-ictal vs. post-ictal: $p = 0.000$; late-ictal vs. post-ictal: $p = 0.000$) bands. The ratio in the gamma band gradually ($p > 0.05$) elevated to a peak from the inter-ictal state to the early-ictal or the late-ictal state, and then sharply declined ($p < 0.05$) to a lower level in the post-ictal period, even lower than that in the inter-ictal section. In the not-seizure-free group, the trend was not observed in any frequency band. The EPLs (including 20 patients) did not show any significant dynamic changes of out/in ratio in chronological order, no matter what grouping methods we used. The RLs showed a completely different trend that demonstrated a significantly steep rise in the four bands (except for delta, $p = 0.098$) during the post-ictal periods regardless of the prognosis.

3.4. Comparisons related to the types of TLEs and EEG ictal onset patterns

The Mann–Whitney test showed that, in the patients with mesial TLE, there was no significant difference in the out/in ratio of the OLs between the seizure-free (15 cases) and not-seizure-free (13 cases) subgroup. In the patients with neocortical TLE, significantly lower values were found in the seizure-free (7 cases) subgroup in the gamma ($p = 0.040$) band under the post-ictal condition.

The Kruskal–Wallis multiple comparison test (in chronological order) showed that the out/in ratio of the OLs in the gamma band declined sharply in the post-ictal stage not only in the seizure-free patients with mesial TLE (vs. early-ictal: $p = 0.000$; vs. late-ictal: $p = 0.001$), but also in the seizure-free patients with neocortical TLE (vs. early-ictal: $p = 0.042$; vs. late-ictal: $p = 0.007$); this difference could not be found in the not-seizure-free patients with both mesial and neocortical TLE.

The Mann–Whitney test showed that, in the 11 patients with low-frequency high-amplitude periodic spikes, no difference was found between the seizure-free and not-seizure-free groups, whereas in the 12 patients with low-voltage fast activities, significantly lower values were found in the seizure-free (5 cases) subgroup in the gamma ($p = 0.042$) band under the post-ictal condition. The Kruskal–Wallis multiple comparison test (in chronological order) showed that the out/in ratio of the OLs in the 5 seizure-free cases with low-frequency high-amplitude periodic spikes only had a slight trend of decline in the gamma band during the post-ictal period ($p = 0.054$), but that in the 5 seizure-free cases with low-voltage fast activities had a significant decline (vs. late-ictal: $p = 0.035$); such a difference could not be found in the not-seizure-free cases in either of the two EEG onset patterns.

Table 2
Significant differences between the lead groups in the different temporal sections.

	OLs vs. EPLs n = 20	OLs vs. RLs n = 20	EPLs vs. RLs n = 20	OLs vs. RLs SF, n = 23	OLs vs. RLs NSF, n = 20
1–4 Hz					
Inter-ictal					p = 0.014
Pre-ictal		p = 0.016			
Early-ictal					
Late-ictal					
Post-ictal					
4–8 Hz					
Inter-ictal		p = 0.033			
Pre-ictal					
Early-ictal					
Late-ictal					p = 0.025
Post-ictal		p = 0.030		p = 0.000	
8–13 Hz					
Inter-ictal		p = 0.018	p = 0.009	p = 0.020	p = 0.004
Pre-ictal		p = 0.003	p = 0.006	p = 0.005	p = 0.030
Early-ictal		p = 0.023		p = 0.031	p = 0.003
Late-ictal		p = 0.000	p = 0.004	p = 0.000	p = 0.006
Post-ictal		p = 0.020		p = 0.001	
13–30 Hz					
Inter-ictal		p = 0.009		p = 0.015	
Pre-ictal		p = 0.014	p = 0.001	p = 0.002	
Early-ictal		p = 0.002	p = 0.026	p = 0.000	p = 0.001
Late-ictal		p = 0.000	p = 0.009	p = 0.000	p = 0.000
Post-ictal				p = 0.031	
30–80 Hz					
Inter-ictal		p = 0.004	p = 0.004	p = 0.000	
Pre-ictal	p = 0.021	p = 0.000		p = 0.000	p = 0.000
Early-ictal		p = 0.000	p = 0.000	p = 0.000	p = 0.000
Late-ictal		p = 0.000	p = 0.000	p = 0.000	p = 0.000
Post-ictal				p = 0.002	

OLs = the onset leads; EPLs = the early propagation leads; RLs = the rest of the leads.

3.5. Outcome prediction

Based on the results of the above analysis, two conditions were combined to predict the EZ. The first condition was that the out/in ratio of the leads within the EZ in the 30–80-Hz band should be no < 1.10 during the early-ictal period and more than that during post-ictal and pre-ictal periods. The second condition was that the correlation coefficient between the out/in ratios of the leads within the EZ and those of the most marked onset lead identified by visual inspection in the five bands during the five periods should be no < 0.5. Any leads confirmed to be in line with the regularity composed of these two conditions were thought to have potential epileptogenicity. More leads met the first condition in the OLs than those in the EPLs and RLs. The number of leads meeting the second condition was not compared because 43 OLs used as reference leads for correlation were included in the 60 leads meeting this condition (see Table 1 and Fig. 3A).

The condition of whether the leads showing the above-mentioned regularity were within the resection range was used to predict surgical outcome, and the results showed that the sensitivity was 91% and the specificity was 70%, p = 0.000 (see Fig. 3B). If the OLs were only required to meet the first condition, the sensitivity was 96% and the specificity was 50%, p = 0.001. There were 11 patients whose OLs did not meet the first condition; among these, 10 were not seizure free (six with low-voltage fast activities: three neocortical TLE and three mesial TLE; three with low-frequency high-amplitude periodic spikes mesial TLE; one with spike or polyspike fast discharges: mesial TLE), and one

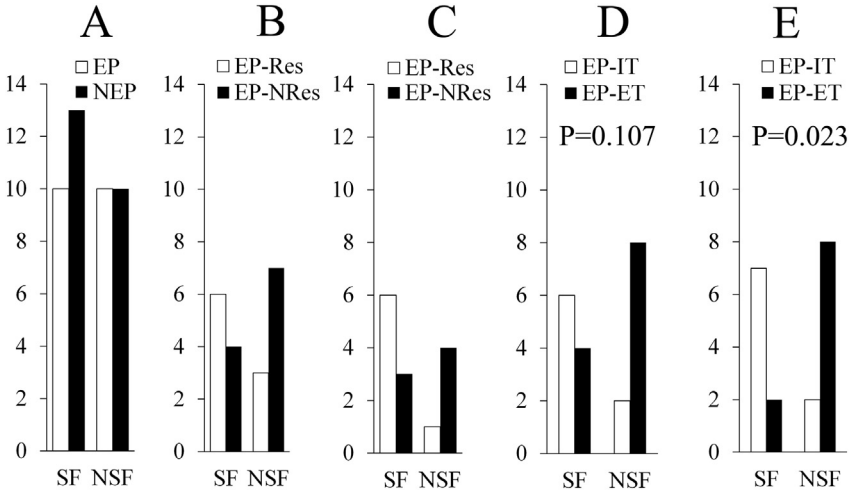

Fig. 2. Relationship between early propagation and surgical outcome. SF = seizure-free; NSF = not-seizure-free.
A. Comparing the difference of the surgical outcome between the patients with and without the early propagation leads. EP = early propagation; NEP = no early propagation.
B. Comparing the difference of the surgical outcome between the patients undergoing and not undergoing the resection of the early propagation region. EP-Res = resection of the early propagation; EP-NRes = no resection of the early propagation.
C. After excluding the patients with the onset leads not showing the first condition that we have given, the comparison just like Fig. 2B was performed again.
D. Comparing the difference of the surgical outcome between the patients with early propagation within 5 s after ictal onset outside and within temporal lobe. EP-ET = early propagation of extra-temporal lobe; EP-IT = early propagation of intra-temporal lobe.
E. Comparing the difference of the surgical outcome between the patients with early propagation within 3 s after ictal onset outside and within temporal lobe.

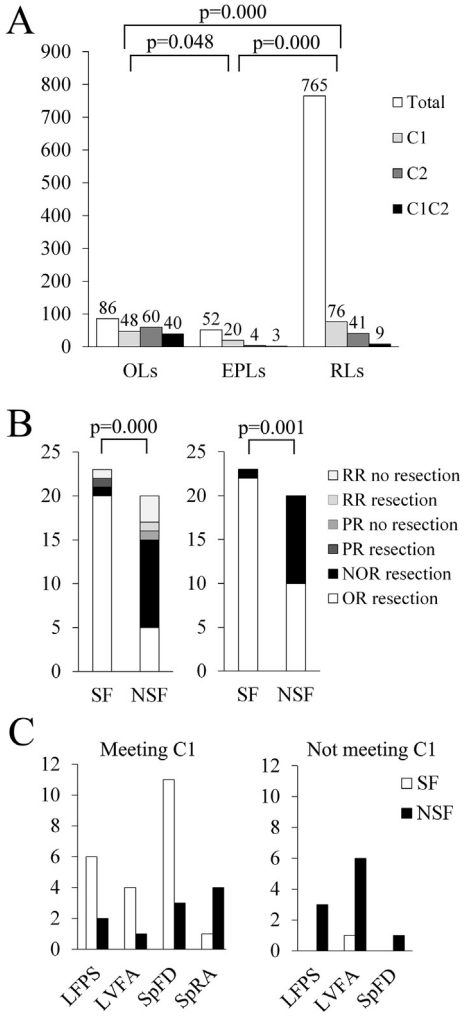

Fig. 3. Relationship between the regularity and the surgical outcome.

A. The distribution of the leads that meet the two conditions that we have pre-established. OLs = the onset leads; EPLs = the early propagation leads; RLs = the rest of the leads; C1 = first condition; C2 = second condition; C1C2 = first condition combined with second condition. We only compared the distribution of the leads that meet the C1 in this study.

B. The detailed distribution of the leads that meet the two conditions in the seizure-free (SF) and not-seizure-free (NSF) groups. The left figure shows the results under the condition of the onset leads meeting the C1 and the other leads meeting the C1 combined with C2. The right figure shows the results under the condition of the onset leads meeting the C1. OR = the onset leads meeting the regularity; NOR = the onset leads not meeting the regularity; PR = the early propagation leads meeting the regularity; RR = the rest of the leads meeting the regularity.

C. The distribution of the surgical outcome in the four EEG onset patterns related to the resection of the onset leads meeting the C1. SF = seizure-free; NSF = not-seizure-free; LFPS = low-frequency high-amplitude periodic spikes; LVFA = low-voltage fast activity; SpFD = spike or polyspike fast discharges; SpRA = spike- or sharp-and-wave rhythmic activity.

was seizure free (with low-voltage fast activities: neocortical TLE). The quantity distribution of the OLs meeting the first condition in the four EEG ictal onset patterns is shown in Fig. 3C.

In the 23 patients with seizure-free, 21 underwent a resection that included all the leads showing regularity. Among these, 20 underwent a complete resection that included the OLs (for an example see Fig. 4); and one (No. 22) underwent a resection that included the OLs (left anterior hippocampus) and EPLs (left anterior middle temporal gyrus). In the other two patients with seizure-free, one (No. 19) had a resection of the OLs (right anterior hippocampus) not including the RLs (left anterior hippocampus and right orbitofrontal gyrus) showing regularity; and one (No. 20) did not have the OLs showing regularity.

In the 20 patients with not-seizure-free, 6 underwent a resection that included all the leads showing regularity. Among these, 5 (No. 1, 24, 43, 13, and 17) underwent a resection that included the OLs, and one (No. 15) underwent a resection that included the OLs (left posterior hippocampus) and the RLs (left anterior hippocampus); 8 patients underwent a resection of the OLs that did not show regularity; 1 patient underwent a resection of the OLs that did not show regularity but not including the RLs showing regularity (for an example, see Fig. 5); 4 patients underwent a resection that did not include either the EPLs (No. 21: left posterior hippocampus and left anterior long gyrus of insular) or the RLs (No. 7: right anterior middle temporal gyrus; No. 29: left precuneus; No. 42: right precuneus) showing regularity.

4. Discussion

New computer-based quantitative EEG analyses have been developed in collaboration with the signal analysis community to expedite EZ detection (Bartolomei et al., 2008; Gnatkovsky et al., 2011; Andrzejak et al., 2012; David et al., 2011; Andrzejak et al., 2015). In recent years, a few groups have begun using an approach based on brain connectivity and graph theory to investigate how the EZ gives rise to network alterations in patients with focal epilepsy. These studies indicate that this network-based approach may add new and valuable information, providing quantitative measures useful either for localizing the EZ or for greatly reducing the number of contacts (Wilke et al., 2010; Panzica et al., 2013; Van Mierlo et al., 2013).

TLE is the most common type of drug-resistant epilepsy in adults, and it commonly requires surgical treatment (Hernández-Ronquillo et al., 2016). There have been some quantitative EEG analyses tested in TLE (Murro et al., 1993; Bartolomei et al., 2008; Seong-Cheol et al., 2015), but the graph theory-based approach is seldom used. Accordingly, we want to use PTE analysis and graph theory to make an active effort to analyze the properties and dynamics of the epileptogenic network giving rise to seizures in patients with drug-resistant TLE.

4.1. Effective connectivity and epileptic network

Functional connectivity and neural network analysis based on SEEG have been used in studying TLE for over 10 years (Bartolomei et al., 2004; Ponten et al., 2007; Bartolomei et al., 2013). The question of what metric is preferable for representing interregional relationships is ultimately a statistical issue, and it also depends on the research of interest (Kida et al., 2014). Phase synchronization of neuronal oscillations has been suggested to underlie the coordination and integration of anatomically distributed processing. To quantify “causal” or directional inter-areal phase-phase interactions, a phase-based measure of effective connectivity is needed (Lobier et al., 2014).

In this study, we selected PTE to construct effective connectivity. There were several reasons for this choice. First, PTE reliably measures directed coupling strength, even in the combined presence of noise and linear mixing. Second, PTE detects interactions between time series across a wide range of underlying interaction lags. Third, PTE is both sample-size and computationally efficient. Finally, PTE can identify frequency band limited information flow (Lobier et al., 2014; Siebenhuehner et al., 2013).

In a weighted and directed graph, nodes have two different degrees, the in-degree and out-degree, which are the sum of incoming and outgoing edge weights, respectively (Kida et al., 2014). Some researchers have used the out-degree to identify the EZ. One study has shown that, during the first 20 s of ictal rhythmic intracranial EEG activity in the 3–20-Hz band, the intracranial EEG contact showing the maximal ictal out-degree was among those visually classified by clinicians as belonging to the seizure onset zone (Van Mierlo et al., 2013). Another study considered the local out- and in-density of each node, defined as the ratio between the sum of node degrees and the total number of vertices in the network (Panzica et al., 2013). The out/in

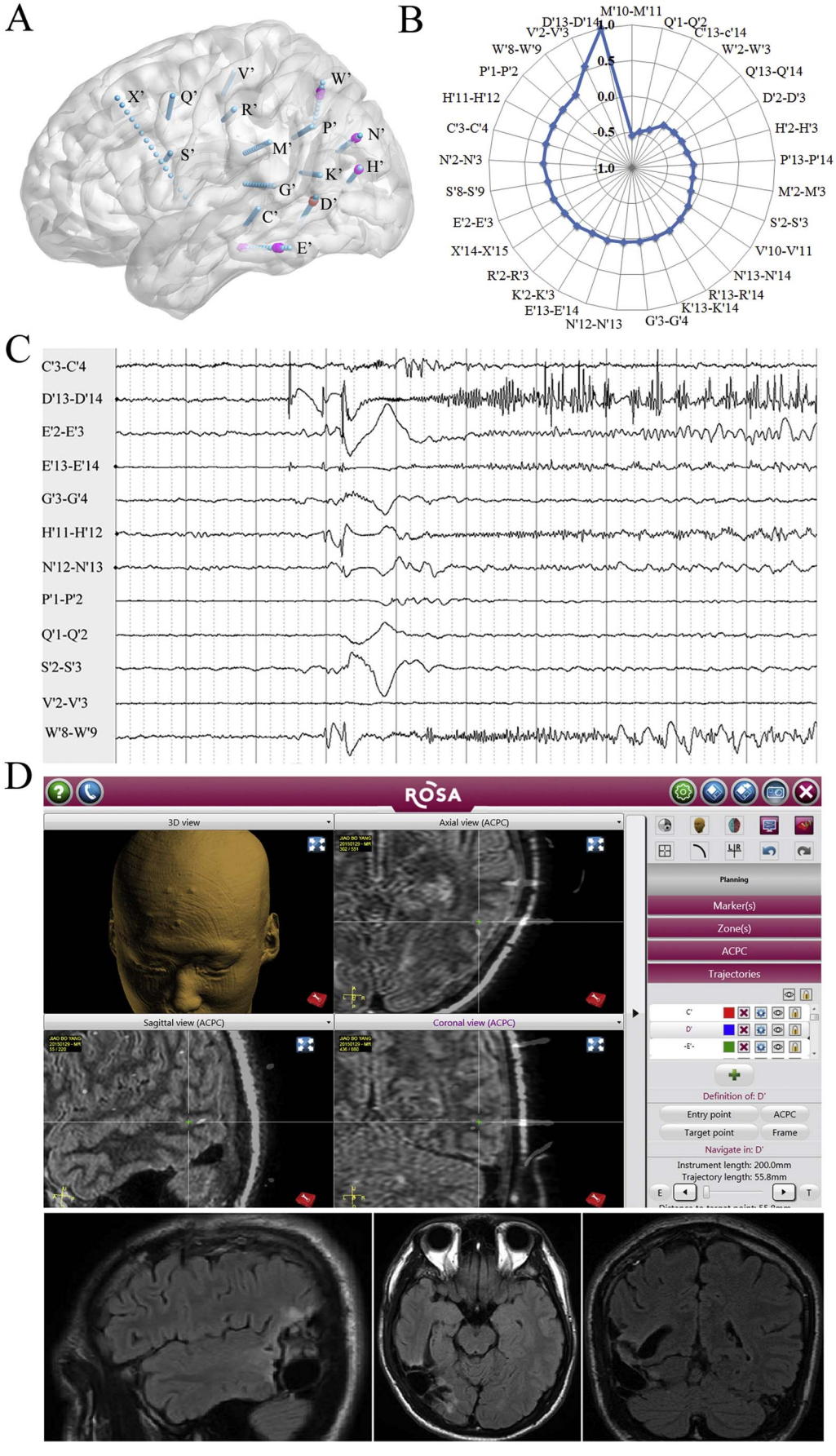

Fig. 4. An example of the surgical outcome prediction in neocortical temporal lobe epilepsies (case: No. 6, Engel's Ia).

A. The schematic diagram of SEEG electrode placement—right view. Red: seizure onset; pink: early propagation. C′3–4: posterior hippocampus; C′13–14: middle temporal gyrus; D′2–3: fusiform gyrus; D′13–14: inferior temporal sulcus; E′2–3: parahippocampus gyrus; E′13–14: inferior temporal gyrus; G′3–4: anterior long gyrus of insular; H′2–3: calcarine fissure; H′11–12: lateral occipital lobe; K′2–3: posterior cingulate gyrus; K′13–14: posterior middle temporal gyrus; M′2–3: anterior long gyrus of insular; M′10–M′11: supermarginal gyrus; N′2–3: precuneus; N′12–13: intraparietal sulcus;N′13–14: angular gyrus; P′1–2: posterior long gyrus of insular; P′13–14: supermarginal gyrus; Q′1–2: middle cingulate gyrus; Q′13–14: posterior middle frontal gyrus; R′2–3: middle cingulate gyrus; R′13–14: precentral gyrus; S′2–3: middle short gyrus of insular; S′8–9: inferior frontal gyrus; V′2–3: sensory supplementary motor area; V′10–11: precentral sulcus; W′2–3: precuneus; W′8–9: superior parietal lobule; X′14–15: middle frontal lobe.

B. Spearman's rank correlation coefficient values quoted on web chart demonstrating the value of the V′1–2 > 0.5 (correlation with D′13–14). The out/in ratio in the 30–80-Hz band during the inter-, pre- early-, late-, and post-ictal periods (not shown in the Fig. 4), D′13–14: 1.21, 1.24, 1.30, 1.57 and 0.75; V′1–2: 0.93, 0.89, 0.84, 0.92, and 0.81.

C. SEEG traces showing the first unequivocal low-voltage fast activities in the D13–D14 in the ictal stage and subsequently in the W′8–9, H′11–12, E′13–14, and E′2–3.

D. Resection of the temporo-occipital junction, not including the W′8–9 (one of the early propagation leads) and the V′1–2 (meeting C2 but not C1). Green +: D13–14.

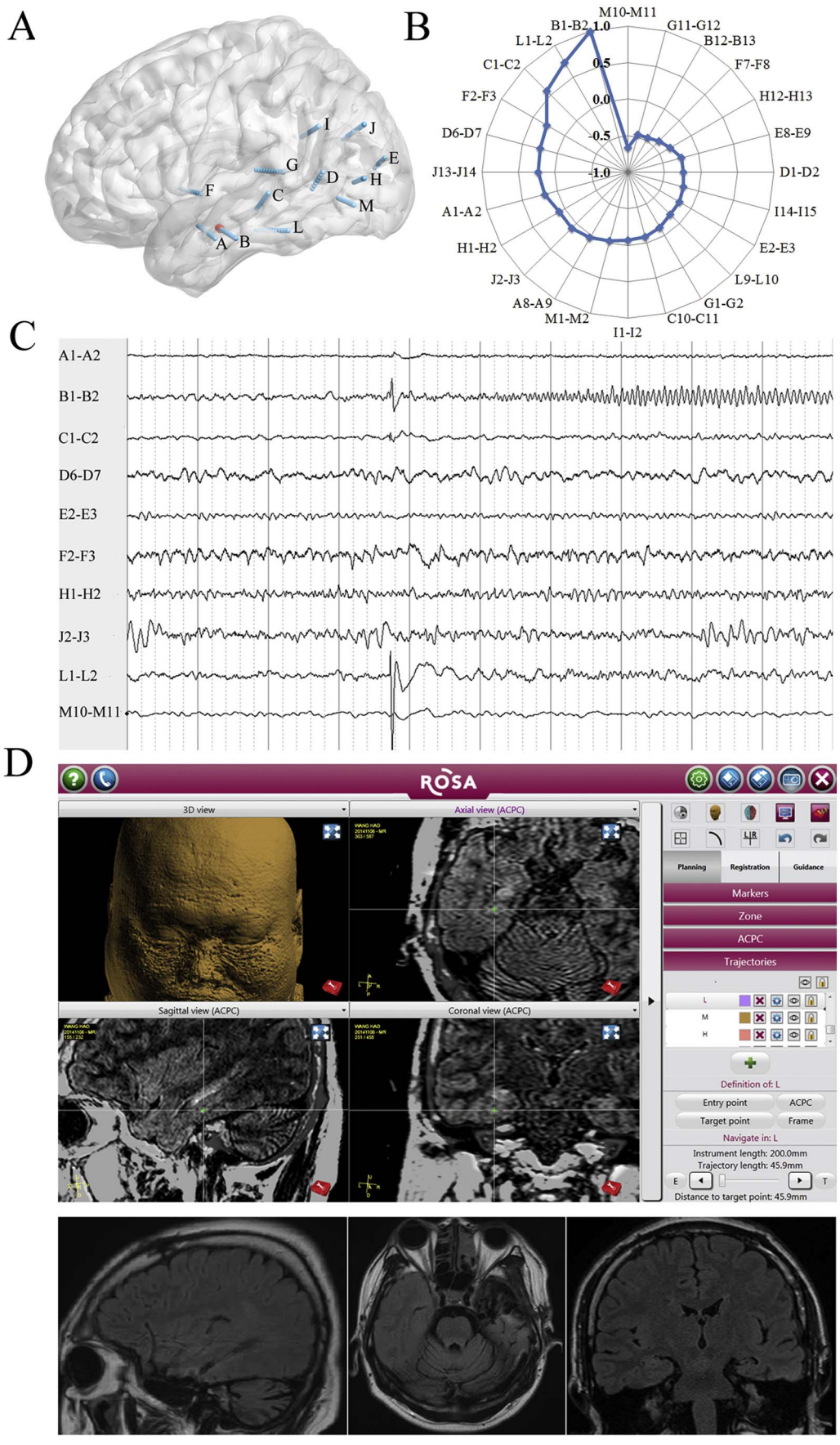

Fig. 5. An example of the surgical outcome prediction in mesial temporal lobe epilepsies (case: No. 25, Engel's Ic).

A. The schematic diagram of SEEG electrode placement—left view. Red color: seizure onset. A1–2: amygdala; A8–9: anterior inferior temporal sulcus; B1–2: anterior hippocampus; B12–13: anterior middle temporal gyrus; C1–2: posterior hippocampus; C10–11: middle temporal gyrus; D6–7: posterior middle temporal gyrus; E2–3: anterior cuneus; E8–9: lateral occipital lobe; F2–3: temporal operculum; F7–8: superior temporal gyrus; G1–2: posterior long gyrus of insular; G11–12: posterior superior temporal gyrus; H1–2: anterior calcarine fissure; H12–13:lateral occipital lobe; I1–2: posterior cingulate gyrus; I14–15: supermarginal gyrus; J1–2: precuneus; J13–14: angular gyrus; L1–2: fusiform gyrus; L9–10: inferior temporal gyrus.

B. Spearman's rank correlation coefficient values quoted on a web chart demonstrating the value of the L1–2 > 0.5 (correlation with B1–2). The out/in ratio in the 30–80-Hz band during the inter-, pre-, early-, late-, and post-ictal periods (not shown in the Fig. 5), B1–2: 1.32, 1.27, 1.26, 1.60, and 0.60; L1–2: 1.23, 1.22, 1.31, 1.32, and 0.81.

C. SEEG traces showing the first unequivocal low voltage fast activities on the B1–2 in the early-ictal stage.

D. Resection of the anterior hippocampus, not including the L1-L2. Green +: L1–2.

ratio used in our study, which is in substantial agreement with the latter study, can overcome the limitation of the varied number of network nodes of each patient.

4.2. Differences of out/in ratio between the three kinds of lead

First of all, we attempted to analyze weather there were significant differences in the out/in ratio between the OLs, EPLs and RLs in the twenty patients with early propagation. Consequently, the difference almost could not be found between the OLs and EPLs. In addition, although there were many differences between the OLs and RLs in these patients, the difference in the out/in ratio during the post-ictal could not be found. We thought that the samples mixed with the two groups of surgical outcome might show reduced statistical effectiveness. Therefore, we made a comparison between the OLs and RLs in the seizure-free and not-seizure-free group, respectively. The results suggested that the real OLs should have lower values of out/in ratio at the post-ictal stage in the frequency bands > 4 Hz. A further analysis between the OLs and EPLs in the two groups of surgical outcome was made, and the results suggested that the lack of such lower values of out/in ratio in the EPLs during the post-ictal section was related to a better outcome.

4.3. Dynamic changes of out/in ratio and frequency bands related to SOZ

Then, we attempted to analyze the dynamic trend of the out/in ratio, and observed which trend was more obvious between the rise during early-ictal stage and the decline under the post-ictal condition. Unexpectedly, the out/in ratio of the OLs of the seizure-free cases in the gamma band under the early-ictal state was not significantly higher than that under the inter-ictal state, and only showed the slightly higher trend (adjusted $p = 0.071$). The sharp decline of the seizure-free cases in the theta, alpha, and gamma bands in the post-ictal stage was much more significant, especially in the gamma band. Of course, this sharp decline may result from lack of continuous EEG signal analysis between the late-ictal and post-ictal temporal sections.

Our findings suggest that the outflow of electrical activities in the EZ is extensively attenuated during the post-ictal stage. Previous studies showed that the temporal target of the epileptogenicity index filter would be between − 15 and 10 s from the ictal onset (Park et al., 2014). Our results strengthened the theory that the post-ictal stage is also an important temporal target to identify EZ, although it is difficult to identify.

A recent study showed that a subset of nodes from SOZ is isolated from the network at seizure onset and becomes more connected with the network toward seizure termination (Khambhati et al., 2015; Burns et al., 2014). Automatic seizure termination is likely due to the fact that a portion of the inhibitory neurons and synapses are upregulated in the seizure-onset cortices (Wen et al., 2015). Another point of view is that focal seizures are terminated by the simultaneous and opposing enhancement of excitation, in addition to post-burst inhibition. A seizure stops when post-burst inhibition becomes large enough to prevent reactivation of excitation (Boido et al., 2014). Our findings may support the latter opinion, because the dynamic changes of the out/in ratio in gamma bands suggested a kind of confrontation between excitation and inhibition.

Our findings showed that EEG activity in the gamma band played a more important role in seizure generation in patients with TLE because the out/in ratio of the OLs in the seizure-free group in this band was significantly higher than that in the other bands during the early- and late-ictal periods, and higher than delta and theta bands during the pre-ictal band. The band that is most significantly related to SOZ is still controversial and may be affected by multiple factors, including the recording equipment, the periods of investigation, and the analysis methods (Park et al., 2012; Park et al., 2014). The gamma and ripple bands between 60 and 200 Hz during the peri-ictal stage were most significantly related to SOZ (Ayala et al., 2011; Modur et al., 2011; Nariai et al., 2011; Ochi et al., 2007; Park et al., 2012; Tito et al., 2009).

4.4. Relationship between early propagation and epileptogenicity

The out/in ratio of the EPLs in the gamma band showed superiority only under the late-ictal condition and not including the pre- and early ictal periods when the OLs showed significantly higher outflow. This suggests that SOZ demonstrates an insidiously earlier gamma activation than the early propagation region. Moreover, the out/in ratio of the EPLs did not show sharp decline in the pos-ictal section, which was very different from the outflow attenuation in the OLs. Great importance should be attached to this phenomenon.

EZ was proposed first by Talairach and Bancaud, who defined it as the “site of the beginning of the epileptic seizures and of their primary organization.” They preferred to use the term “primary organization of the epileptic seizure,” rather than the term “early seizure spread,” because an “early” or a “late” SEEG change cannot be assessed in terms of either seconds or tens of seconds (Kahane et al., 2006). However, “early spread’ proved to be useful in clinical application; for example, statistically high ‘Epileptogenicity Index’ values corresponded to structures involved early in the ictal process and producing rapid discharges at seizure onset (Bartolomei et al., 2008). Stimulation elicited enhanced gamma band activity at early spread sites, which was highly coherent with the onset zone (Lega et al., 2015). Latencies of spread maybe related to the degree of integrity of inhibition in these areas, with early spread as a possible indicator of secondary epileptogenesis (Götz-Trabert et al., 2008). Our results also show that early extratemporal propagation within 3 s rather than 5 s after EEG onset suggested worse surgical outcome when comparing early intratemporal spreading. Despite all this, we still think that spreading latency is a phenomenon which can be affected by many factors, and there should be better parameters that demonstrate the essence of epileptogenicity.

Our findings showed that OLs showing the typical dynamic changes of the out/in ratio was a determining factor of surgical outcome and that the early propagation with similar dynamic patterns can also demonstrate higher epileptogenicity, which may be regarded as the primary organization. However, after excluding the cases with atypical onset, a complete resection of the early propagation was still unrelated to the surgical outcome, which suggested that some other regions demonstrating this kind of pattern might be omitted. As it is easier to omit extratemporal propagation than intratemporal spreading, patients with early extratemporal propagation have a worse surgical outcome.

4.5. Differences related to the types of TLE and to the EEG ictal onset patterns

We found that the decline of the out/in ratio in the gamma band of the OLs in the neocortical TLE group might be a more valid predictor of outcome than that in the mesial TLE group, and the same results were shown between the low-voltage fast activities and the low-frequency high-amplitude periodic spikes group.

We think that out/in ratio analysis of the ictal onset patterns may reveal the essence of the difference among the types of TLE. As is known, low-frequency high-amplitude periodic spikes and low-voltage fast activities are two separate ictal depth EEG ictal onset patterns often recorded in presurgical patients with mesial TLE. Our results suggested a better surgical outcome if the outflow of the low-voltage fast activities onset in the gamma band decreased more obviously under the postictal condition. Curiously, such a relation was not shown in the low-frequency high-amplitude periodic spikes group. This finding may be related to histopathological difference between these two groups. Evidence suggests the mechanisms generating seizures with low-frequency high-amplitude periodic spikes and low-voltage fast activities onset are distinct, including differential involvement of hippocampal and extra-hippocampal sites (Memarian et al., 2015). Seizures with

low-frequency high-amplitude periodic spikes onset have greater hippocampal cell loss, which may be related to not only burst style of ictal onset pattern, but also insufficient attenuation in the post-ictal stage. This phenomenon should be examined by expanding the sample size and frequency bandwidth in a further study.

Onset of seizures with low-voltage fast activities are associated with high-frequency oscillations in the ripple band (80–200 Hz), whereas seizures with low-frequency high-amplitude periodic spikes initiate in the hippocampus and tend to remain focal, with predominant fast ripples (250–500 Hz). Nevertheless, the frequency band higher than 160 Hz may not be significantly related to the SOZs (Park et al., 2014). Hence, the 80–160-Hz frequency band should be included to analyze the difference of outflow among the types of ictal onset patterns.

4.6. EZ prediction

We used a regularity that included two given conditions for EZ prediction in the 43 TLE patients. So far, the accuracy of EZ prediction can only be tested by surgical outcomes. Recent studies have focused on whether causal source activity, calculated from each of the seizures individually, is completely within the clinical SOZ in seizure-free patients; however, the models were seldom tested in patients with bad outcomes (Varotto et al., 2012; Wilke et al., 2010; Van Mierlo et al., 2013; Antony et al., 2013). Our approach proved to be both highly sensitive and specific for EZ identification, even if the real SOZ is not covered by the depth electrodes. This approach should be used in combination with visual inspection because the temporal sections and the contacts of the leads must be selected by an expert electroencephalographist.

We found that the leads with a dynamic trend of the out/in ratio similar to that of the typical OLs were significantly related to SOZs. Adding the second condition as a restriction, the sensitivity of surgical outcome prediction greatly increased; however, the specificity moderately decreased because the first given condition was not so strict that 36% EPLs and 10% RLs could match it, but most of them were not within the range of resection. If the OLs were only required to meet the first condition, the sensitivity slightly increased to 96%, but the specificity sharply decreased to 50%.

The surgical outcome was influenced not only by EZ identification but also by the coverage of electrode implantation and the range of resection (Park et al., 2014). For example, patient No. 1 still had some palpitation auras after selective amygdalo-hippocampectomy. The risk of recurrence may be high if the temporal pole is speared under the condition of no electrodes being implanted into this region. Patient No. 24 had frequent seizures after a selective amygdalo-hippocampectomy, not including lingual gyrus and posterior cingulate gyrus, which are the early propagation regions, but the dynamic changes of the out/in ratio in these sites did not meet the second given condition. He was seizure free after the second surgical resection, including the whole hippocampus and most of basal temporal and anterior temporal lobes. Patient No. 22 had two types of seizure onset from the superior temporal gyrus or superior temporal gyrus together with insula, but the range of resection did not include the insula.

4.7. Limitations

There are a few limitations of the methodology of this study in addition to a small sample size. First, it was a retrospective study, in which the designs of electrode implantation were not perfectly standardized, with the result that a few conventional sites of implantation, for example, temporal pole and entorhinal (Chabardès et al., 2005; Bartolomei et al., 2004), were omitted in some of the patients. Second, the selection of the leads was restricted by visual inspection, and the selected leads were representative, although the quantity was smaller, which may result in a partial loss of EEG signal. Third, the late-ictal temporal section was difficult to define because of the variability of the seizure spreading. Fourth, the higher frequency band (above 80 Hz) was not included in this study because our EEG instruments had a lower sampling rate.

5. Conclusions

The determination of the epileptogenicity of brain regions potentially involved in seizure generation is crucial pre-surgical work in patients suffering from ‘atypical’ TLE. In the present study, we have shown that a significant difference of the out/in ratio (mainly in the gamma band) distinguishes the OLs from the RLs, not only during the inter-ictal, pre-ictal, and ictal periods but also during the post-ictal stage. The real OLs have a characteristic dynamic trend of this ratio: slight rise during the early-ictal period and sharp decline in the post-ictal stage. This dynamic trend is demonstrated in the different types of TLE and EEG onset patterns, which suggests that it could be a general law in accurate localization of the EZ, although the predictive validity of the surgical outcome may be different in the subgroups. Our preliminary results also imply that similarity of the dynamic patterns of the out/in ratio in the onset regions, rather than spreading latency, might be the key discriminating factor of epileptogenicity.

In brief, this study indicates that a PTE and graph theory-based approach may add new and valuable information, providing efficient quantitative measures useful for localizing the EZ.

Conflict of interest

The authors declare no competing financial interests.

Acknowledgments

This work was supported by the China Postdoctoral Science Foundation (2015M571069), Beijing Postdoctoral Research Foundation 2015-ZZ-61, Beijing Municipal Science & Technology Commission (Z161100002616016) and National Natural Science Foundation of China (81671285).

The authors would also like to thank Professor Meichen Yu from VU University Medical Center for the advice about methodology and improving the readability of the paper.

References

Andrzejak, R.G., Schindler, K., Rummel, C., 2012. Nonrandomness, nonlinear dependence, and nonstationarity of electroencephalographic recordings from epilepsy patients. Phys. Rev. E Stat. Nonlinear Soft Matter Phys. 86, 2745–2756. http://dx.doi.org/10.1103/PhysRevE.86.046206.

Andrzejak, R.G., David, O., Gnatkovsky, V., Wendling, F., Bartolomei, F., Francione, S., Kahane, P., Schindler, K., De, C.M., 2015. Localization of epileptogenic zone on presurgical intracranial EEG recordings: toward a validation of quantitative signal analysis approaches. Brain Topogr. 28, 832–837. http://dx.doi.org/10.1007/s10548-014-0380-8.

Antony, A.R., Alexopoulos, A.V., González-Martínez, J.A., Mosher, J.C., Jehi, L., Burgess, R.C., So, N.K., Galán, R.F., 2013. Functional connectivity estimated from intracranial EEG predicts surgical outcome in intractable temporal lobe epilepsy. PLoS One 8, e77916. http://dx.doi.org/10.1371/journal.pone.0077916.

Ayala, M., Cabrerizo, M., Jayakar, P., Adjouadi, M., 2011. Subdural EEG classification into seizure and nonseizure files using neural networks in the gamma frequency band. J. Clin. Neurophysiol. Off. Publ. Am. Electroencephalogr. Soc. 28, 20–29. http://dx.doi.org/10.1097/WNP.0b013e31820512ee.

Barba, C., Barbati, G., Minotti, L., Hoffmann, D., Kahane, P., 2007. Ictal clinical and scalp-EEG findings differentiating temporal lobe epilepsies from temporal ‘plus’ epilepsies. Brain 130, 1957–1967. http://dx.doi.org/10.1093/brain/awm108.

Bartolomei, F., Wendling, F., Régis, J., Gavaret, M., Guye, M., Chauvel, P., 2004. Pre-ictal synchronicity in limbic networks of mesial temporal lobe epilepsy. Epilepsy Res. 61, 89–104. http://dx.doi.org/10.1016/j.eplepsyres.2004.06.006.

Bartolomei, F., Chauvel, P., Wendling, F., 2008. Epileptogenicity of brain structures in human temporal lobe epilepsy: a quantified study from intracerebral EEG. Brain 131 (Pt 7), 1818–1830. http://dx.doi.org/10.1093/brain/awn111.

Bartolomei, F., Bettus, G., Stam, C.J., Guye, M., 2013. Interictal network properties in mesial temporal lobe epilepsy: a graph theoretical study from intracerebral recordings. Clin. Neurophysiol. 124, 2345–2353. http://dx.doi.org/10.1016/j.clinph.2013.06.003.

Boccaletti, S., Latora, V., Moreno, Y., Chavez, M., Hwang, D.U., 2006. Complex networks:

structure and dynamics. Phys. Rep. 424, 175–308.
Boido, D., Gnatkovsky, V., Uva, L., Francione, S., de Curtis, M., 2014. Simultaneous enhancement of excitation and postburst inhibition at the end of focal seizures. Ann. Neurol. 76, 826–836. http://dx.doi.org/10.1002/ana.24193.
Burns, S.P., Santaniello, S., Yaffe, R.B., Jouny, C.C., Crone, N.E., Bergey, G.K., Anderson, W.S., Sarma, S.V., 2014. Network dynamics of the brain and influence of the epileptic seizure onset zone. Proc. Natl. Acad. Sci. U. S. A. 111, 5321–5330. http://dx.doi.org/10.1073/pnas.1401752111.
Chabardès, S., Kahane, P., Minotti, L., Tassi, L., Grand, S., Hoffmann, D., Louisbenabid, A., 2005. The temporopolar cortex plays a pivotal role in temporal lobe seizures. Brain 128, 1818–1831. http://dx.doi.org/10.1093/brain/awh512.
Coito, A., Plomp, G., Genetti, M., Abela, E., Wiest, R., Seeck, M., Michel, C.M., Vulliemoz, S., 2015. Dynamic directed interictal connectivity in left and right temporal lobe epilepsy. Epilepsia 56, 207–217. http://dx.doi.org/10.1111/epi.12904.
Dauwan, M., van der Zande, J.J., van Dellen, E., Sommer, I.E., Scheltens, P., Lemstra, A.W., Stam, C.J., 2016. Random forest to differentiate dementia with Lewy bodies from Alzheimer's disease. Alzheimers Dement. (Amst) 4, 99–106. http://dx.doi.org/10.1016/j.dadm.2016.07.003.
David, O., Blauwblomme, T., Job, A.S., Chabardès, S., Hoffmann, D., Minotti, L., Kahane, P., 2011. Imaging the seizure onset zone with stereo-electroencephalography. Brain 134, 2898–2911. http://dx.doi.org/10.1093/brain/awr238.
Engel Jr, J., 1993. Update on surgical treatment of the epilepsies. Summary of the Second International Palm Desert Conference on the Surgical Treatment of the Epilepsies (1992). Neurology 43, 1612–1617.
Gnatkovsky, V., Francione, S., Cardinale, F., Mai, R., Tassi, L., Lo Russo, G., De Curtis, M., 2011. Identification of reproducible ictal patterns based on quantified frequency analysis of intracranial EEG signals. Epilepsia 52, 477–488. http://dx.doi.org/10.1111/j.1528-1167.2010.02931.x.
Gnatkovsky, V., De Curtis, M., Pastori, C., Cardinale, F., Lo Russo, G., Mai, R., Nobili, L., Sartori, I., Tassi, L., Francione, S., 2014. Biomarkers of epileptogenic zone defined by quantified stereo-EEG analysis. Epilepsia 55, 296–305. http://dx.doi.org/10.1111/epi.12507.
Götz-Trabert, K., Hauck, C., Wagner, K., Fauser, S., Schulze-Bonhage, A., 2008. Spread of ictal activity in focal epilepsy. Epilepsia 49, 1594–1601. http://dx.doi.org/10.1111/j.1528-1167.2008.01627.x.
Haneef, Z., Lenartowicz, A., Yeh, H.J., Levin Jr., H.S., E., J., Stern, J.M., 2014. Functional connectivity of hippocampal networks in temporal lobe epilepsy. Epilepsia 55, 137–145. http://dx.doi.org/10.1111/epi.12476.
Hernández-Ronquillo, L., Buckley, S., Ladino, L.D., Wu, A., Moien-Afshari, F., Rizvi, S.A., Téllez-Zenteno, J.F., 2016. How many adults with temporal epilepsy have a mild course and do not require epilepsy surgery? Epileptic Disord. 18, 137–147. http://dx.doi.org/10.1684/epd.2016.0822.
Kahane, P., Landré, E., Minotti, L., Francione, S., Ryvlin, P., 2006. The Bancaud and Talairach view on the epileptogenic zone: a working hypothesis. Epileptic Disord. 8 (Suppl. 2), S16–26.
Khambhati, A.N., Davis, K.A., Oommen, B.S., Chen, S.H., Lucas, T.H., Litt, B., Bassett, D.S., 2015. Dynamic network drivers of seizure generation, propagation and termination in human neocortical epilepsy. PLoS Comput. Biol. 11, 749–759. http://dx.doi.org/10.1371/journal.pcbi.1004608.
Kida, T., Tanaka, E., Kakigi, R., 2014. Multi-dimensional dynamics of human electromagnetic brain activity. Front. Hum. Neurosci. 9 (365). http://dx.doi.org/10.3389/fnhum.2015.00713.
Lega, B., Dionisio, S., Flanigan, P., Bingaman, W., Najm, I., Nair, D., Gonzalez-Martinez, J., 2015. Cortico-cortical evoked potentials for sites of early versus late seizure spread in stereoelectroencephalography. Epilepsy Res. 115, 17–29. http://dx.doi.org/10.1016/j.eplepsyres.2015.04.009.
Lobier, M., Siebenhühner, F., Palva, S., Palva, J.M., 2014. Phase transfer entropy: a novel phase-based measure for directed connectivity in networks coupled by oscillatory interactions. NeuroImage 85 (Pt 2), 853–872. http://dx.doi.org/10.1016/j.neuroimage.2013.08.056.
Memarian, N., Madsen, S.K., Macey, P.M., Fried, I., Engel Jr., J., Thompson, P.M., Staba, R.J., 2015. Ictal depth EEG and MRI structural evidence for two different epileptogenic networks in mesial temporal lobe epilepsy. PLoS One 10, e0123588. http://dx.doi.org/10.1371/journal.pone.0123588.
Modur, P.N., Zhang, S., Vitaz, T.W., 2011. Ictal high-frequency oscillations in neocortical epilepsy: implications for seizure localization and surgical resection. Epilepsia 52, 1792–1801. http://dx.doi.org/10.1111/j.1528-1167.2011.03165.x.
Murro, A.M., Yong, D.P., King, D.W., Gallagher, B.B., Smith, J.R., Meador, K.J., Littelton, W., 1993. Localization of temporal lobe seizures with quantitative EEG. Electroencephalogr. Clin. Neurophysiol. 86, 88–93.
Nariai, H., Nagasawa, T., Juhász, C., Sood, S., Chugani, H.T., Asano, E., 2011. Statistical mapping of ictal high-frequency oscillations in epileptic spasms. Epilepsia 52, 63–74. http://dx.doi.org/10.1111/j.1528-1167.2010.02786.x.
Ochi, A., Otsubo, H., Donner, E.J., Elliott, I., Iwata, R., Funaki, T., Akizuki, Y., Akiyama, T., Imai, K., Rutka, J.T., Snead, O.C., 2007. Dynamic changes of ictal high-frequency oscillations in neocortical epilepsy: using multiple band frequency analysis. Epilepsia 48, 286–296. http://dx.doi.org/10.1111/j.1528-1167.2007.00923.x.
Panzica, F., Varotto, G., Rotondi, F., Spreafico, R., Franceschetti, S., 2013. Identification of the epileptogenic zone from stereo-EEG signals: a connectivity-graph theory approach. Front. Neurol. 4, 175. http://dx.doi.org/10.3389/fneur.2013.00175.
Park, S.C., Lee, S.K., Che, H., Chung, C.K., 2012. Ictal high-gamma oscillation (60–99 Hz) in intracranial electroencephalography and postoperative seizure outcome in neocortical epilepsy. Clin. Neurophysiol. 123, 1100–1110. http://dx.doi.org/10.1016/j.clinph.2012.01.008.
Park, S.C., Sang, K.L., Chung, C.K., 2014. Peri-ictal broadband electrocorticographic activities between 1 and 700 Hz and seizure onset zones in 18 patients. Clin. Neurophysiol. 125, 1731–1743. http://dx.doi.org/10.1016/j.clinph.2014.01.022.
Perucca, P., Dubeau, F., Gotman, J., 2014. Intracranial electroencephalographic seizure-onset patterns: effect of underlying pathology. Brain 137, 183–196. http://dx.doi.org/10.1093/brain/awt299.
Ponten, S.C., Bartolomei, F., Stam, C.J., 2007. Small-world networks and epilepsy: graph theoretical analysis of intracerebrally recorded mesial temporal lobe seizures. Clin. Neurophysiol. 118, 918–927. http://dx.doi.org/10.1016/j.clinph.2006.12.002.
Seong-Cheol, P., Kun, L.S., Chun Kee, C., 2015. Quantitative peri-ictal electrocorticography and long-term seizure outcomes in temporal lobe epilepsy. Epilepsy Res. 109C, 169–182. http://dx.doi.org/10.1016/j.eplepsyres.2014.10.005.
Siebenhuehner, F., Lobier, M., Palva, S., Palva, M., 2013. Phase transfer entropy: a novel measure for effective connectivity among neuronal oscillations. BMC Neurosci. 14, 305. http://dx.doi.org/10.1186/1471-2202-14-S1-P305.
Singh, S., Sandy, S., Wiebe, S., 2015. Ictal onset on intracranial EEG: do we know it when we see it? State of the evidence. Epilepsia 56, 1629–1638. http://dx.doi.org/10.1111/epi.13120.
Stam, C.J., 2014. Modern network science of neurological disorders. Nat. Rev. Neurosci. 15, 683–695. http://dx.doi.org/10.1038/nrn3801.
Tito, M., Cabrerizo, M., Ayala, M., Jayakar, P., Adjouadi, M., 2009. Seizure detection: an assessment of time- and frequency-based features in a unified two-dimensional decisional space using nonlinear decision functions. Clin. Neurophysiol. 26, 381–391. http://dx.doi.org/10.1097/WNP.0b013e3181c29928.
Van Mierlo, P., Carrette, E., Hallez, H., Raedt, R., Meurs, A., Vandenberghe, S., Van Roost, D., Boon, P., Staelens, S., Vonck, K., 2013. Ictal-onset localization through connectivity analysis of intracranial EEG signals in patients with refractory epilepsy. Epilepsia 54, 1409–1418. http://dx.doi.org/10.1111/epi.12206.
Varotto, G., Tassi, L., Franceschetti, S., Spreafico, R., Panzica, F., 2012. Epileptogenic networks of type ii focal cortical dysplasia: a stereo-EEG study. NeuroImage 61, 591–598. http://dx.doi.org/10.1016/j.neuroimage.2012.03.090.
Wen, B., Qian, H., Feng, J., Ge, R.J., Xu, X., Cui, Z.Q., Zhu, R.Y., Pan, L.S., Lin, Z.P., Wang, J.H., 2015. A portion of inhibitory neurons in human temporal lobe epilepsy are functionally upregulated: an endogenous mechanism for seizure termination. CNS Neurosci. Ther. 21, 204–214. http://dx.doi.org/10.1111/cns.12336.
Wilke, C., Van, D.W., Kohrman, M., He, B., 2010. Neocortical seizure foci localization by means of a directed transfer function method. Epilepsia 51, 564–572. http://dx.doi.org/10.1111/j.1528-1167.2009.02329.x.